Properties of Intracellular Ca²⁺ Waves Generated by a Model Based on Ca²⁺-Induced Ca²⁺ Release

Geneviève Dupont and Albert Goldbeter

Faculté des Sciences, Université Libre de Bruxelles, B-1050 Brussels, Belgium

ABSTRACT Cytosolic Ca²⁺ waves occur in a number of cell types either spontaneously or after stimulation by hormones, neurotransmitters, or treatments promoting Ca²⁺ influx into the cells. These waves can be broadly classified into two types. Waves of type 1, observed in cardiac myocytes or *Xenopus* oocytes, correspond to the propagation of sharp bands of Ca²⁺ throughout the cell at a rate that is high enough to permit the simultaneous propagation of several fronts in a given cell. Waves of type 2, observed in hepatocytes, endothelial cells, or various kinds of eggs, correspond to the progressive elevation of cytosolic Ca²⁺ throughout the cell, followed by its quasi-homogeneous return down to basal levels. Here we analyze the propagation of these different types of intracellular Ca²⁺ waves in a model based on Ca²⁺-induced Ca²⁺ release (CICR). The model accounts for transient or sustained waves of type 1 or 2, depending on the size of the cell and on the values of the kinetic parameters that measure Ca²⁺ exchange between the cytosol, the extracellular medium, and intracellular stores. Two versions of the model based on CICR are considered. The first version involves two distinct Ca²⁺ pools sensitive to inositol 1,4,5-trisphosphate (IP₃) and Ca²⁺, respectively, whereas the second version involves a single pool sensitive both to Ca²⁺ and IP₃ behaving as co-agonists for Ca²⁺ release. Intracellular Ca²⁺ waves occur in the two versions of the model based on CICR, but fail to propagate in the one-pool model at subthreshold levels of IP₃. For waves of type 1, we investigate the effect of the spatial distribution of Ca²⁺-sensitive Ca²⁺ stores within the cytosol, and show that the wave fails to propagate when the distance between the stores exceeds a critical value on the order of a few μm. We also determine how the period and velocity of the waves are affected by changes in parameters measuring stimulation, Ca²⁺ influx into the cell, or Ca²⁺ pumping into the stores. For waves of type 2, the numerical analysis indicates that the best qualitative agreement with experimental observations is obtained for phase waves. Finally, conditions are obtained for the occurrence of "echo" waves that are sometimes observed in the experiments.

INTRODUCTION

A large variety of cells respond to extracellular signals such as hormones and neurotransmitters by a temporally and spatially organized variation in intracellular Ca²⁺ corresponding to the occurrence of Ca²⁺ oscillations or to the propagation of intracellular Ca²⁺ waves (Berridge and Galione, 1988; Berridge, 1990, 1993; Cuthbertson, 1989; Cuthbertson and Cobbold, 1991; Meyer and Stryer, 1991; Tsien and Tsien, 1990; Dupont and Goldbeter, 1992; Amundson and Clapham, 1993; Fewtrell, 1993; Jaffe, 1993; Rooney and Thomas, 1993; Berridge and Dupont, 1994). Depending on the cell type or on the extracellular agonist, Ca²⁺ oscillations vary in period (from a few seconds to tens of minutes), shape (transient spikes or sinusoidal oscillations), and sensitivity to different drugs.

The shape and propagation velocity of Ca²⁺ waves also seem to differ from one cell type to another. In some cell types such as cardiac cells (Takamatsu and Wier, 1990), waves propagate as sharp bands with velocities and frequencies that are high enough to allow for the simultaneous propagation of distinct fronts in a given individual cell. The latter

type of wave has been called type 1 for convenience (Dupont and Goldbeter, 1992). In contrast (see Fig. 1), waves of type 2, referred to as "tides" by Tsien and Tsien (1990), have been defined as ones in which the level of Ca²⁺ progressively rises along the entire cell before returning to the basal level in a quasi-homogeneous manner. This behavior has been reported for eggs (Jaffe, 1983, 1993; Cheek et al., 1993; Galione et al., 1993), hepatocytes (Thomas et al., 1991), and endothelial cells (Jacob, 1990).

The appearance of type 1 or type 2 waves depends on the balance between the kinetics of Ca²⁺ exchange processes and the dimension of the cell, so that a continuum exists between the two types of waves that differ only by their appearance. Thus type 2 waves are observed in small cells whose kinetics are slow enough to generate very wide Ca²⁺ fronts, whereas Ca²⁺ waves of type 1 are favored in large cells when the kinetics are so rapid that the Ca²⁺ front remains narrow with respect to cellular dimensions. A similar distinction between the two kinds of waves was pointed out by Meyer (1991). On the other hand, spiral waves are sometimes observed in *Xenopus* oocytes (Lechleiter et al., 1991) and cardiac myocytes (Lipp and Niggli, 1993). Intercellular Ca²⁺ waves involving transport through gap junctions have also been reported in glial (Cornell-Bell et al., 1990; Charles et al., 1991) and airway epithelial cells (Boitano et al., 1992).

The mechanism of Ca²⁺ oscillations and waves has been extensively studied from both an experimental and a theoretical point of view. It is well established that inositol 1,4,5-trisphosphate (IP₃), synthesized in response to external stimulation, induces the release of Ca²⁺ from intracellular
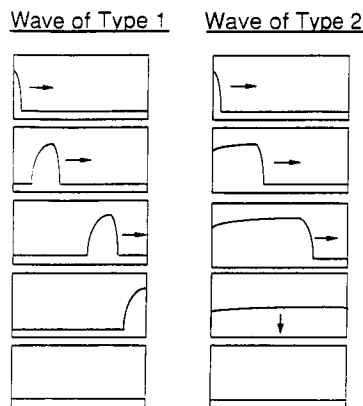
Wave of Type 1   Wave of Type 2

FIGURE 1 Schematic representation of the two types of intracellular Ca^{2+} waves. Waves of type 1 propagate as sharp bands (left side), while waves of type 2 propagate as tides (right side).

stores (Berridge, 1993). A first class of models for Ca^{2+} oscillations rely on an oscillating level of IP_3, due either to the activation of its synthesizing enzyme, phospholipase C (PLC), by Ca^{2+} (Meyer and Stryer, 1988, 1991), or to a hypothetical, positive feedback process accompanied by negative regulation exerted by the activated protein kinase C on the G-protein that mediates the extracellular signal to PLC (Woods et al., 1987; Cuthbertson and Chay, 1991).

The fact that Ca^{2+} oscillations can be induced by nonmetabolizable analogues of IP_3 suggests, in contrast, that the oscillatory mechanism lies beyond the process of IP_3 synthesis (Wakui et al., 1989). Thus, in a number of cell types, a key role in the oscillations is played by the positive feedback exerted by cytosolic Ca^{2+} on Ca^{2+} release from intracellular stores (Kort et al., 1985; Busa et al., 1985; Wakui et al., 1990; Thomas et al, 1991). Such a regulation, known as Ca^{2+}-induced Ca^{2+} release (CICR), is at the core of models for Ca^{2+} oscillations in a variety of excitable or nonexcitable cells (Kuba and Takeshita, 1981; Goldbeter et al., 1990; Dupont et al., 1991; Somogyi and Stucki, 1991; Wong et al., 1992; Jafri et al., 1992; De Young and Keizer, 1992; Atri et al., 1993; Dupont and Goldbeter, 1993). Among all these models, an important distinction can be made as to the phenomenon responsible for the termination of a Ca^{2+} spike. While some of these models assume that the partial depletion of the Ca^{2+} store is sufficient to bring down Ca^{2+} release (Kuba and Takeshita, 1981; Goldbeter et al., 1990; Dupont et al., 1991; Somogyi and Stucki, 1991), others incorporate the inhibition of Ca^{2+} release by the IP_3 receptor at Ca^{2+} concentrations higher than those producing CICR (Jafri et al., 1992; De Young and Keizer, 1992; Atri et al., 1993). It should be noted that periodic IP_3 changes could passively follow Ca^{2+} oscillations because of some coupling mechanism such as the activation of IP_3 synthesis or degradation by cytosolic Ca^{2+} (Swillens and Mercan, 1990; Dupont et al., 1991).

In a given cell type, Ca^{2+} oscillations and waves are closely related and most likely rely on the same feedback mechanisms. Therefore, the species whose diffusion plays a

primary role in Ca^{2+} wave propagation could be IP_3 (Meyer and Stryer, 1991) and/or Ca^{2+}. In cardiac cells, where a depolarization-induced increase in Ca^{2+} influx from the extracellular medium is sufficient to trigger the propagation of a Ca^{2+} wave, the major role is certainly played by Ca^{2+}. In the same manner, tert-butyl hydroperoxyde, a compound that bypasses IP_3 formation, can initiate wave propagation in hepatocytes (Thomas et al., 1991). In Xenopus oocytes however, Ca^{2+} and IP_3 are both required for the propagation of Ca^{2+} waves. In the latter case it appears that Ca^{2+} excitability depends on IP_3 receptor channels that are sensitive to the surrounding concentration of cytosolic Ca^{2+} (Lechleiter and Clapham, 1992; DeLisle and Welsh, 1992).

This paper is devoted to a theoretical study of Ca^{2+} wave propagation in two versions of a model based on CICR previously proposed for Ca^{2+} oscillations. In the first version of the model (Goldbeter et al., 1990; Dupont et al., 1991), two Ca^{2+} pools respectively sensitive to IP_3 and Ca^{2+} are considered. The second version (Dupont and Goldbeter, 1993) assumes the existence of a single pool sensitive to Ca^{2+} and IP_3 behaving as co-agonists for Ca^{2+} release. To emphasize the fact that the self-amplified process of CICR release is each time at the core of the mechanism of oscillations and waves, these two forms of regulation are respectively referred to as IP_3-insensitive and IP_3-sensitive CICR (Dupont and Goldbeter, 1993).

In the following, after recalling the main features of the one- and two-pool versions of the model in the next section, we determine in later sections the conditions for the occurrence of waves of type 1 and 2, successively. For both types of waves, we treat separately the cases of a solitary front (i.e., the response to transient stimulation) and of sustained waves. We illustrate type 1 waves by means of two different simulations aimed at reproducing the situations of cardiac myocytes and of Xenopus oocytes. Of primary importance are the spatial distribution of CICR domains and the kinetic parameters which determine the period and half-width of repetitive Ca^{2+} spikes. We then focus on qualitative aspects of waves of type 2 and show that "echo" waves can occur in some conditions. Such a phenomenon can be related to experimental observations on Ca^{2+} waves in ascidian eggs (Speksnijder et al., 1990). We discuss these results in the final section and emphasize that, beyond some differences, the one- and two-pool versions of the model based on CICR exhibit similar behavior when the effect of diffusion is taken into account.

ONE- AND TWO-POOL VERSIONS OF THE MODEL FOR CA²⁺ OSCILLATIONS BASED ON CICR

In building models for Ca^{2+} oscillations based on CICR, the question arises as to the molecular entity where activation of Ca^{2+} release by cytosolic Ca^{2+} occurs. In some cells such as Xenopus oocytes (Lechleiter and Clapham, 1992; DeLisle and Welsh, 1992) or Purkinje cells (Bezprozvanny et al., 1991; Finch et al., 1991), Ca^{2+} and IP_3 behave as co-agonists

for Ca²⁺ release. On the other hand, the existence of two types of Ca²⁺ pools, one sensitive to IP₃ (possessing IP₃ receptors) and one sensitive to Ca²⁺ (possessing caffeine/ryanodine receptors), has been demonstrated in other cells such as adrenal chromaffin cells (Stauderman and Murawsky, 1991; Meldolesi et al., 1990), pituitary cells (Law et al., 1990), Purkinje neurons (Walton et al., 1991), parotid acinar cells (Foskett and Wong, 1991), smooth muscle cells (Matsumoto et al., 1990; Blatter and Wier, 1992), hepatocytes (Nathanson et al., 1992, 1994), and sea urchin eggs (Galione et al., 1993; Lee et al., 1993). The control of Ca²⁺-sensitive, IP₃-insensitive pools could be more complex than what has been considered so far, as it has recently been discovered that the Ca²⁺ channel function of the ryanodine receptor can be modulated by cyclic ADP-ribose (Galione, 1992; Galione et al., 1993; Lee et al., 1993).

Two-pool version of the model based on CICR

The existence of two distinct types of Ca²⁺ stores is taken into account in the two-pool model based on CICR. A detailed analysis of that model has been presented elsewhere (Goldbeter et al., 1990; Dupont et al., 1991). Here, we simply recall the kinetic equations of the model, together with the definition of the parameters. As the IP₃ level is assumed to remain constant as long as external stimulation is maintained, the model contains only two variables, namely cytosolic (Z) and intravesicular (Y) Ca²⁺. When taking into account the two-dimensional diffusion of cytosolic Ca²⁺ within a planar section through the cell, the time evolution of cytosolic and intravesicular Ca²⁺ is given by the following differential equations (see Fig. 2 A):

$$\frac{\partial Z}{\partial t} = V_{in} - V_2 + V_3 + k_f Y - kZ + D_Z\left(\frac{\partial^2 Z}{\partial x^2} + \frac{\partial^2 Z}{\partial y^2}\right) \quad (1)$$

$$\frac{dY}{dt} = V_2 - V_3 - k_f Y$$

with

$$V_{in} = \nu_0 + \nu_1\beta \quad (2)$$

$$V_2 = V_{M2}\frac{Z^n}{K_2^n + Z^n} \quad (3)$$

$$V_3 = V_{M3}\frac{Y^m}{K_R^m + Y^m}\frac{Z^p}{K_A^p + Z^p} \quad (4a)$$

In these equations, V_{in} represents the total, constant entry of Ca²⁺ into the cytosol; it includes the background influx from the extracellular medium, ν_0 (this term may include a possible contribution from some IP₃-insensitive intracellular stores), as well as the IP₃-stimulated Ca²⁺ influx $\nu_1\beta$ from the IP₃-sensitive store (β is the degree of saturation of the IP₃ receptor); V_2 and V_3 are, respectively, the rates of pumping into and release from the Ca²⁺-sensitive store with V_{M2} and V_{M3} denoting the maximum rates of these processes; K_2, K_R, and K_A are the threshold constants for pumping, release, and activation, while n, m, and p are the Hill coefficients char-
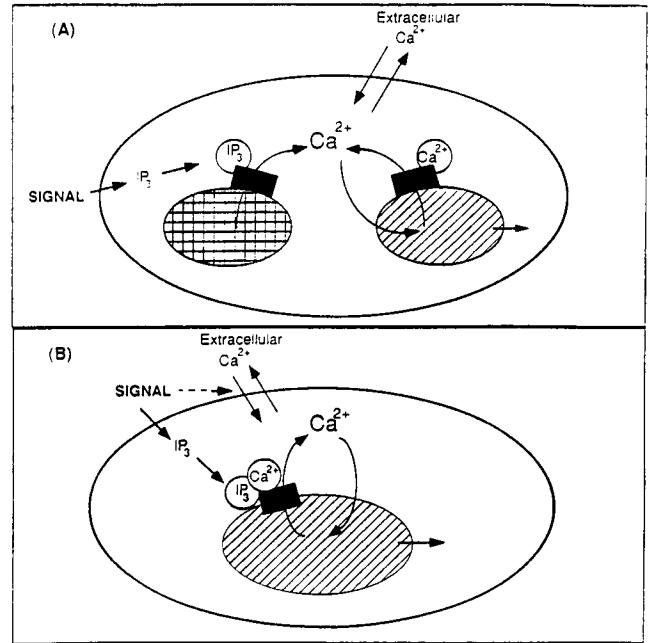

FIGURE 2 Schematic representation of the two-pool (A) and one-pool (B) models for Ca²⁺ oscillations based on CICR. In both cases, the level of IP₃, which increases with the level of external stimulation, is assumed to remain constant. Cytosolic Ca²⁺ activates the release of Ca²⁺ from an IP₃-insensitive, Ca²⁺-sensitive store (A) or from a Ca²⁺ and IP₃-sensitive store (B). The two variables of the minimal model are Z, the cytosolic Ca²⁺ concentration, and Y, the concentration of Ca²⁺ in the pool sensitive to Ca²⁺ (A) or to IP₃ and Ca²⁺ (B) (see Goldbeter et al. (1990), Dupont et al. (1991), and Dupont and Goldbeter (1993) for detailed presentation and analysis of the two versions of the CICR model).

acterizing these processes; $k_f Y$ and kZ refer to the passive efflux from the Ca²⁺-sensitive store and from the cytosol; D_Z is the diffusion coefficient for cytosolic Ca²⁺. The rate of release of Ca²⁺ from the Ca²⁺-sensitive store, V_3, incorporates the activation by cytosolic Ca²⁺ at the basis of CICR, but not the inhibition seen at higher Ca²⁺ levels.

One-pool version of the model based on IP₃-sensitive CICR

When only one type of Ca²⁺ pool is considered, with IP₃ and Ca²⁺ acting as co-agonist for Ca²⁺ release (Fig. 2 B), the model based on CICR defined by Eq. 1 can still account for the existence and for the main properties of Ca²⁺ oscillations (Dupont and Goldbeter, 1993). The kinetic equations describing the evolution of cytosolic Ca²⁺ and of Ca²⁺ in the store sensitive to IP₃ and Ca²⁺ are then only slightly modified. To account for the fact that the same receptor/channel is activated by both IP₃ and Ca²⁺, the term V_3, which now represents the Ca²⁺ release from the unique Ca²⁺- and IP₃-sensitive store, is given by:

$$V_3 = \beta V_{M3}\frac{Y^m}{K_R^m + Y^m}\frac{Z^p}{K_A^p + Z^p} \quad (4b)$$

where β represents the degree of saturation by IP₃ of this

"bi-activated" receptor and V_{M3} the maximum rate of release. The constant Ca^{2+} influx into the cytosol is still given by Eq. (2) but the meaning of $\nu_1\beta$ has changed: it now represents a stimulus-activated Ca^{2+} influx from the extracellular medium into the cytosol. The consideration of such a regulated Ca^{2+} entry, which is supported by recent experimental data (Putney, 1991; Hoth and Penner, 1992; Randriamampita and Tsien, 1993; Parekh et al., 1993), allows one to keep the property that the mean Ca^{2+} level increases with the degree of stimulation. With regard to oscillations the two versions of the CICR model mainly differ by the amplitude of the first Ca^{2+} spike and by its latency, i.e., the time that separates that spike from the onset of stimulation (Dupont and Goldbeter, 1993).

PROPAGATING CA^{2+} FRONTS AND SUSTAINED WAVES OF TYPE 1

We have previously shown that the two-pool model based on CICR can account for the propagation of solitary fronts of cytosolic Ca^{2+} of type 1, in one (Dupont et al., 1991) or two (Dupont and Goldbeter, 1992) spatial dimensions. In these simulations, parameter values were chosen so as to obtain a periodicity of the order of 1 s when stimulation is maintained. When cytosolic Ca^{2+} is elevated at one extremity of the cell, a sharp band of increased Ca^{2+} is then seen to propagate towards the other extremity with a velocity of about 100 μm s^{-1}.

Propagating Ca^{2+} fronts: influence of the distance between Ca^{2+} pools

If Ca^{2+} waves result from the sequential activation of Ca^{2+}-sensitive Ca^{2+} stores distributed across the cell (Berridge, 1990; Dupont et al., 1991) the phenomenon must be markedly influenced by the spatial distribution of Ca^{2+} pools. This question can be conveniently investigated by means of computer simulations. The two-pool model has been adopted for such a study, given that in cardiac myocytes, which are the prototype of cells ex-

hibiting waves of type 1, IP$_3$ does not seem necessary to induce the propagation of Ca^{2+} waves (Endo and Iino, 1990) even if IP$_3$ has been shown to cause contraction of skinned cardiomyofibers (Kijima et al., 1993). In fact, when $\beta = 0$ or $\nu_1 = 0$, the two-pool model reduces to a model containing a single Ca^{2+} pool sensitive to cytosolic Ca^{2+}. Then the main influx of Ca^{2+} into the cytosol, besides CICR, is the one that originates from the extracellular medium (ν_0).

Let us start with the propagation of solitary fronts after transient stimulation. We shall consider in turn a continuous and a nonhomogeneous distribution of Ca^{2+} pools. A first
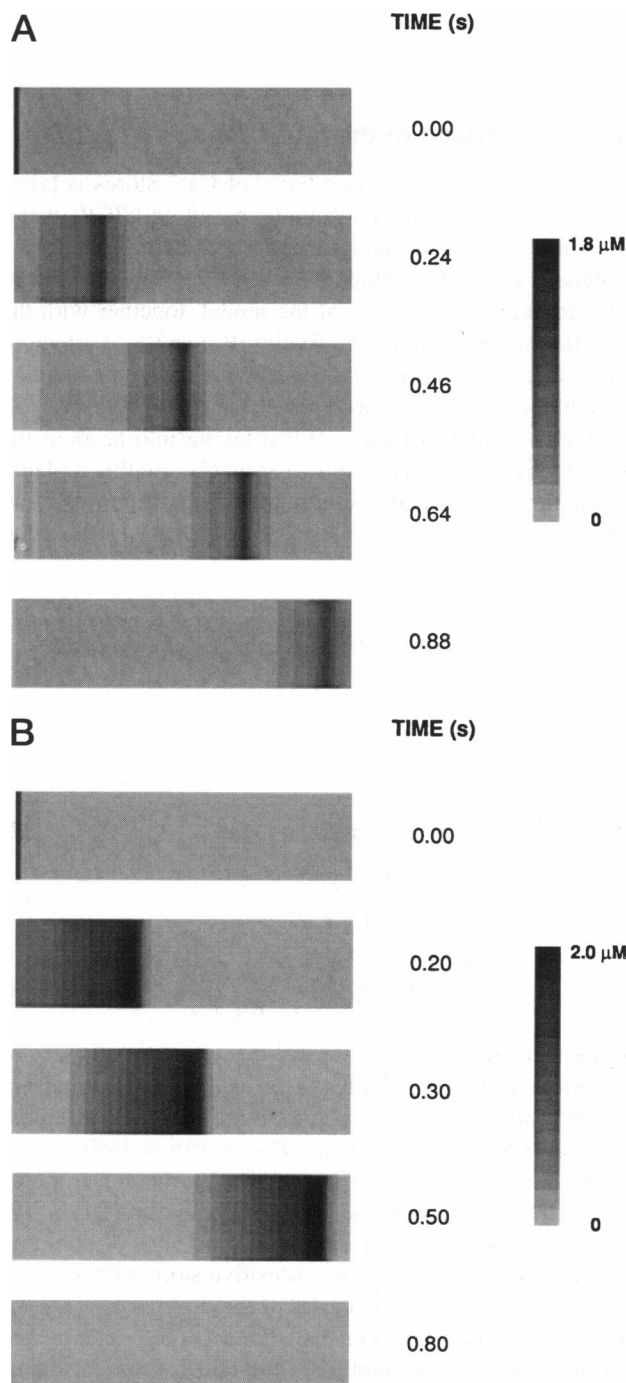

FIGURE 3 Comparison between Ca^{2+} fronts propagating in (A) a system where the CICR domains are supposed to be equidistantly distributed throughout the cell, and (B) a system where CICR occurs in a homogeneous manner over the whole cell. The results are obtained by numerical simulation of the two-pool model based on CICR defined by Eqs. 1–4a. An inhomogeneous distribution of Ca^{2+} stores favors the appearance of a sharp Ca^{2+} front resembling those experimentally observed in cardiac cells. In both panels, the cell considered is 120 × 33 μm; to simulate the diffusion process, the cell is represented as a mesh of 99 × 30 points. For (A), 13 Ca^{2+} pools, each of which occupies four vertical rows of that mesh, are equidistantly distributed throughout the cell. In both cases, the cell is transiently stimulated by raising initially the level of cytosolic Ca^{2+} up to 1.3 μM in the two extreme rows on the left. Everywhere else, the cell is assumed to be initially at stable steady state. Parameter values are: (A) $\nu_0 = 2.5$ μM s^{-1}, $\nu_1 = 0$, $V_{M2} = 80$ μM s^{-1}, $K_2 = 1$ μM, $V_{M3} = 455$ μM s^{-1}, $K_R = 2$ μM, $K_A = 1.0$ μM, $k = 10$ s^{-1}, $k_f = 1$ s^{-1}, $D_Z = 400$ μm^2 s^{-1}, and (B) $\nu_0 = 1.5$ μM s^{-1}, $\nu_1 = 0$, $V_{M2} = 90$ μM s^{-1}, $K_2 = 0.9$ μM, $V_{M3} = 455$ μM s^{-1}, $K_R = 2$ μM, $K_A = 0.9$ μM, $k = 8$ s^{-1}, $k_f = 1$ s^{-1} and $D_Z = 400$ μm^2 s^{-1}. Moreover, as in all subsequent figures, $n = m = 2$, and $p = 4$

difference between the spatial patterns generated in these two cases pertains to the width of the front. As shown by the comparison between Fig. 3, *A* and *B*, a discrete distribution of stores favors the appearance of much sharper bands of increased Ca²⁺. When discrete Ca²⁺ pools are distributed along the cell, the propagation of the front is brought about by the sequential firing of the successive stores while in regions between stores, Ca²⁺ diffuses passively and tends to return towards its (stable) steady-state level given by $Z_0 = v_0/k$ (see, e.g., Goldbeter et al., 1990).

Another difference between the waves obtained with a homogeneous or discrete distribution of Ca²⁺ pools pertains to the relationship between the stimulation level and the velocity of front propagation. As already shown by Sneyd et al. (1993) in the case of a unique, continuous Ca²⁺ pool distributed all over the cell, the speed of a solitary Ca²⁺ front increases with the intensity of stimulation in agreement with the empirical Luther's equation (Tyson and Keener, 1988):

$$v_{prop} = K\sqrt{kD} \qquad (5)$$

where K is a constant depending on the system, D the diffusion coefficient for the propagator species (in the present case: Z, cytosolic Ca²⁺), and k an apparent first-order rate constant for the autocatalytic production of the propagator. Increasing stimulation ($v_1\beta$) leads to an increase in the rate of autocatalytic production of Z and thus to an acceleration of the front. Sneyd et al. (1993) have shown that the velocity of the front may increase by more than a factor of three when increasing the stimulation level and/or the extracellular Ca²⁺ concentration. Numerical simulations in one (Sneyd et al., 1993) or two spatial dimensions (data not shown) confirm these analytical predictions.

In the case of discrete Ca²⁺ stores, the propagation velocity markedly depends on the distance between successive Ca²⁺ pools (as illustrated in Fig. 7 below for the case of sustained Ca²⁺ waves), and only slightly on the stimulation strength (Fig. 4). Indeed, whatever the stimulus, nearly the same amount of Ca²⁺ is released from the Ca²⁺ pool nearest from the initiation site; the time for this Ca²⁺ increase to diffuse to the next CICR site then depends on the distance between the pools. This result, which is a theoretical prediction, has not yet been corroborated by any direct observation on cardiac myocytes. Also shown in Fig. 4 is the fact that in the model, the latency of the Ca²⁺ front decreases with the level of the stimulus. This point has previously been studied in this model in the absence of Ca²⁺ diffusion (Dupont et al., 1990).

In agreement with experimental observations in cardiac cells (Takamatsu and Wier, 1990) and oocytes (Girard et al., 1992) and with the usual behavior of excitable systems, two fronts started at opposite ends of the cell annihilate each other upon collision (Fig. 5).

Sustained Ca²⁺ waves of type 1

The preceding results pertain to the propagation of Ca²⁺ fronts generated in response to transient stimulation, the stimulus being maintained only for a short period of time in
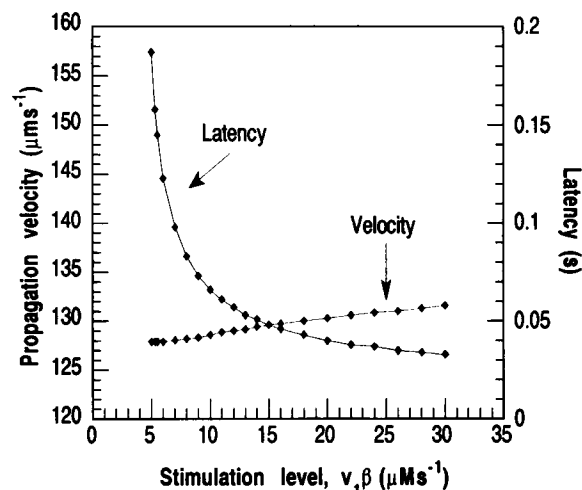

FIGURE 4   Dependence of the propagation velocity and latency of a Ca²⁺ front of type 1 on the level of stimulation in the case of a discrete distribution of Ca²⁺-sensitive Ca²⁺ pools. The propagation velocity is much less dependent upon the level of stimulation than in the case where CICR domains are present throughout the whole cell. As expected from the study of the model in the absence of diffusion, the latency of the front decreases with the level of stimulation. Latency is here defined as the time required to reach the maximum of the first Ca²⁺ spike near the site of stimulation. The points have been obtained by numerical simulation of the model based on CICR, defined by Eqs. 1–4a. The dimension of the cell is 120×24 μm and for simulating diffusion the system is discretized into a grid of 100×30 points. The system is initially at the stable steady state in the absence of stimulation. Stimulation is applied in a transient manner, through an exponentially decreasing term ($v_1\beta e^{-3t}$) added to the first equation of system (1) in the first three rows of points. The cell is assumed to possess 17 equidistant, 3.6 μm-wide Ca²⁺ stores. Parameter values are: $v_0 = 2.496$ μM s⁻¹, $v_1 = 0$, $V_{M2} = 80$ μM s⁻¹, $K_2 = 1$ μM, $V_{M3} = 455$ μM s⁻¹, $K_R = 2$ μM, $K_A = 1.01$ μM, $k = 10$ s⁻¹, $k_f = 1$ s⁻¹ and $D_Z = 400$ μm² s⁻¹.

comparison with the time necessary for the front to propagate from one cell extremity to the other. Transient stimuli do not allow one to account for the simultaneous propagation of two Ca²⁺ fronts often observed in myocytes (Takamatsu and Wier, 1990; Lipp and Niggli, 1993) or *Xenopus* oocytes (Girard et al., 1992; Camacho and Lechleiter, 1993). This phenomenon results from the periodic operation of the Ca²⁺ signaling system because of continuous stimulation.

As myocytes and *Xenopus* oocytes differ in many respects, we have examined successively the situation of Ca²⁺ fronts propagating at high velocity ($\sim$100 μm s⁻¹) in relatively small systems, as in cardiac cells, and the case of slower waves that propagate over much larger areas, as in *Xenopus* oocytes. In both cases, numerical simulations provide insights into properties of the waves such as their shape, velocity, or period. The two-dimensional geometry considered will be rectangular for myocytes and square-shaped for oocytes.

Modeling Ca²⁺ waves in cardiac cells: dependence on the distance between CICR domains

As shown in Fig. 6, sustained Ca²⁺ waves can be obtained in the model based on CICR in the presence of persistent
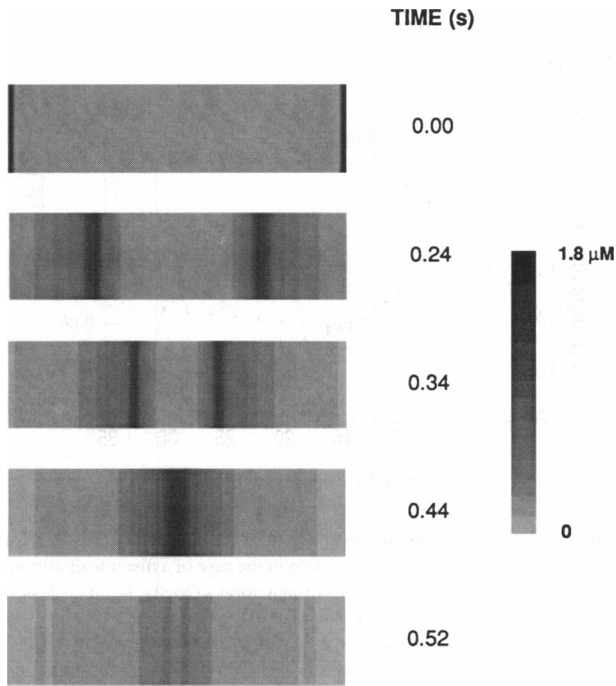
FIGURE 5   Annihilation of two Ca^{2+} fronts of type 1 propagating in opposite directions. The results are obtained by numerical simulation of the model based on CICR defined by Eqs. 1–4a. Conditions and parameter values are as in Fig. 3 A, except that the cell is transiently stimulated on both extremities by raising initially the level of cytosolic Ca^{2+} up to 1.3 μM in the two extreme rows at each end.
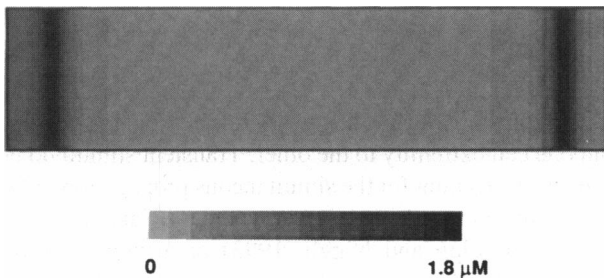

FIGURE 6   Modeling the simultaneous propagation of two Ca^{2+} fronts of type 1 in cardiac myocytes. The figure has been obtained by numerical simulations of the model based on CICR defined by Eqs. 1–4a with $v_0 = 3.4$ μM s^{-1}, $V_{M2} = 80$ μM s^{-1}, $K_2 = 1$ μM, $V_{M3} = 455$ μM s^{-1}, $K_R = 2$ μM, $K_A = 1$ μM, $k = 10$ s^{-1}, $k_f = 1$ s^{-1} and $D_Z = 400$ μm^2 s^{-1}. In these conditions, the period equals 1.27 s and the propagation velocity 116 μm s^{-1}; these values are in good agreement with experimental observations on wave propagation in cardiac myocytes (Kort et al., 1985; Takamatsu and Wier, 1990; Lipp and Niggli, 1993, 1994). The dimension of the cell is 160 × 40 μm and for simulating diffusion the system is discretized into a grid of 132 × 40 points. 17 Ca^{2+} stores are spaced at equal intervals; the stores and the intervals occupy four vertical rows of the grid, and are thus ~4.85 μm wide. The stimulation ($v_1\beta = 4.3$ μM s^{-1}) is constantly applied in the first four rows of points, i.e., in the first, left pool.

stimulation. Successive Ca^{2+} fronts periodically (T ~ 1.3 s) start from the left extremity of the cell, which is continuously stimulated, and propagate toward the other extremity with a velocity of the order of 120 μm s^{-1}. Such values for the period and velocity match those observed for Ca^{2+} waves in

cardiac myocytes (Kort et al., 1985; Takamatsu and Wier, 1990; Lipp and Niggli, 1993, 1994).

In agreement with the experimental results, the wavelength, i.e., the distance between two successive fronts, is slightly lower than the typical cell length. This theoretical result was only obtained in the case of an inhomogeneous distribution of Ca^{2+} pools. Indeed, if one considers that these stores are homogeneously distributed in the cytosol, the successive fronts cannot be sufficiently narrow to remain distinct from each other; the spatio-temporal structure then generated by the model qualitatively differs from experimental observations. The conditions used to generate the wave in Fig. 6 hold with the fact that the sarcoplasmic reticulum, which serves as Ca^{2+} pool, possesses a spatially inhomogeneous structure.

We have seen in Fig. 4 above that when Ca^{2+} pools are assumed to be distributed in the cell in a discrete manner, the model based on CICR predicts only a slight increase of the front propagation velocity when increasing the transient stimulation. In contrast, the spacing between the Ca^{2+} pools considerably affects the period and the propagation velocity of the waves. To allow for the possibility that CICR occurs in discrete locations but nevertheless involves a single Ca^{2+} pool, we may refer to the distance between CICR domains rather than between Ca^{2+} pools. A domain could represent a cluster of Ca^{2+}-activated Ca^{2+} channels and could be related to the sites where Ca^{2+} sparks (Cheng et al., 1993), focal release (Lipp and Niggli, 1994), or hot spots (Parker and Yao, 1991) are observed.

As expected intuitively, the speed is maximal when CICR is homogeneously distributed over the whole cell, whereas the velocity decreases in a quasi-linear manner with the distance between two successive CICR domains (Fig. 7).
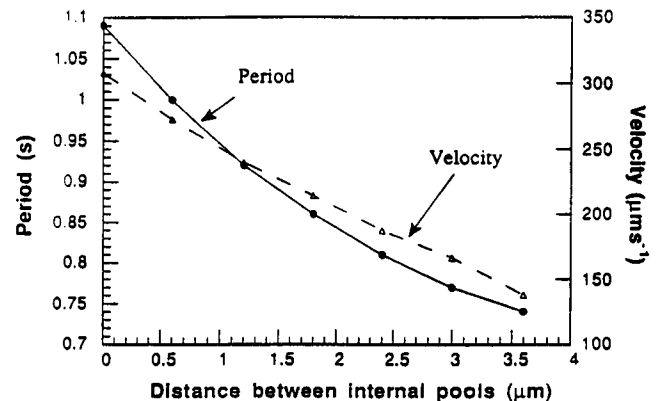

FIGURE 7   Dependence of the period and velocity of Ca^{2+} waves of type 1 on the distance between Ca^{2+}-sensitive Ca^{2+} stores (or CICR domains). The points have been obtained by numerical simulations of Eqs. 1–4a. The dimensions of the cell are 120 × 24 μm, and for simulating diffusion the system is discretized into a grid of 200 × 60 points. Constant stimulation is applied in the first Ca^{2+}-sensitive store of the system at the left extremity. Each Ca^{2+}-sensitive store occupies six vertical rows of the grid and is thus 3.6 μm wide; the number of stores depends on the distance that separates them. Parameter values are: $v_0 = 4$ μM s^{-1}, $v_1\beta = 3$ μM s^{-1}, $V_{M2} = 80$ μM s^{-1}, $K_2 = 1$ μM, $V_{M3} = 455$ μM s^{-1}, $K_R = 2$ μM, $K_A = 1.0$ μM, $k = 10$ s^{-1}, $k_f = 1$ s^{-1}, and $D_Z = 400$ μm^2 s^{-1}.

Interestingly, the period also decreases when these domains get further away from each other. Wave propagation stops if the distance between CICR domains exceeds a critical value on the order of 4 μm for the situation considered in Fig. 7. This critical value, which holds with the distance that separates portions of the sarcoplasmic reticulum in myocytes (Moses and Delcarpio, 1983; Stern, 1992), is about 10 times larger than the critical distance of 0.35 μm predicted by Meyer and Stryer (1991) for the suppression of Ca²⁺ wave propagation in a model based on a CICR mechanism.

The preceding results, which pertain to the situation encountered in cardiac cells, have been obtained by using a value of 400 μm² s⁻¹ for the Ca²⁺ diffusion coefficient (Kushmerick and Podolsky, 1969; Whitaker and Irvine, 1984; Cheer et al., 1987; Donnahue and Abercrombie, 1987; Backx et al., 1989; Girard et al., 1992). The latter value differs from the value close to 40 μm² s⁻¹ recently measured in a cytosolic extract from *Xenopus* oocytes (Allbritton et al., 1992), which we shall use in the next section to model Ca²⁺ wave propagation in oocytes. It should be stressed that such a lower estimate of the Ca²⁺ diffusion coefficient does not permit one to account for the observations in cardiac cells. In that case indeed, sharp Ca²⁺ fronts of type 1 cannot propagate at sufficiently high velocities for values of the kinetic parameters that yield a period of oscillations on the order of 1 s. The measurement of the lower value for the Ca²⁺ diffusion coefficient in *Xenopus* oocytes could be explained by the large Ca²⁺ buffering capacity of the preparation considered. It would be interesting to determine the Ca²⁺ diffusion coefficient in cardiac myocytes in physiological conditions.

Modeling Ca²⁺ waves in *Xenopus* oocytes: dependence on stimulation, external Ca²⁺, and rate of Ca²⁺ pumping into intracellular stores

It has been shown that the model based on CICR defined by Eqs. 1–4a can account for the existence of sustained concentric or spiral Ca²⁺ waves resembling the ones observed in *Xenopus* oocytes (Girard et al., 1992). By choosing the low value for the Ca²⁺ diffusion coefficient (40 μm² s⁻¹) recently measured by Allbritton et al. (1992) and values for the kinetic parameters 60 times lower than the ones used by Girard et al. (1992), the waves obtained in the present case are characterized by a longer period and a lower propagation velocity (Fig. 8) than in the study of the latter authors. As the system is supposed to be sufficiently large (1000 × 1000 μm), two fronts can be seen to propagate simultaneously in one cell. The waves are of type 1 according to the criteria outlined above.

The theoretical approach provides an easy way to investigate the effect of altering various factors on the waves generated by CICR. As many experiments have been performed in *Xenopus* oocytes, we will use the situation illustrated in Fig. 8 as a starting point for our investigations, except that we have assumed that the IP₃-sensitive store is located at the left extremity in the entire two first rows (and not only in their central part as in Fig. 8) to avoid the effects due to curvature.
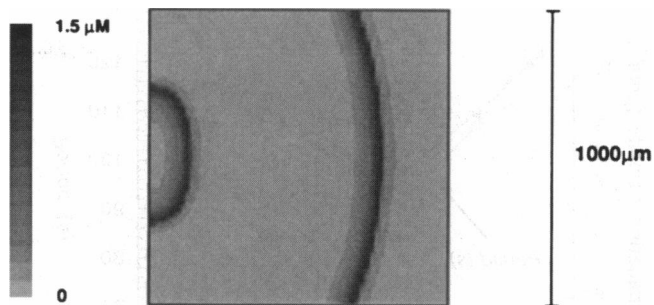

FIGURE 8   Modeling Ca²⁺ waves of type 1 in *Xenopus* oocytes. The figure has been obtained by numerical simulations of the two-pool model based on CICR defined by Eqs. 1–4a with ν_0 = 3.1 μM min⁻¹, V_{M2} = 65 μM min⁻¹, K_2 = 1 μM, V_{M3} = 455 μM min⁻¹, K_R = 2 μM, K_A = 0.9 μM, k = 10 μM min⁻¹, k_f = 1 min⁻¹ and D_Z = 40 μm² s⁻¹. In these conditions, the period equals 83 s and the propagation velocity, 7.8 μm s⁻¹. The dimension of the cell is 1000 × 1000 μm. For simulating diffusion the system is discretized into a grid of 64 × 64 points. Constant stimulation ($\nu_1\beta$ = 0.12 μM min⁻¹) is applied in the central part of the first two rows of points, i.e., in boxes (1,22) to (1,42) and (2,22) to (2,42).

The most straightforward parameter to alter is the stimulation level that is given by $\nu_1\beta$ in the present model (Eq. 2). Recall that we have assumed in this study that the IP₃-stimulated influx is localized in a specific region near the plasma membrane. Fig. 9 *A* shows that in the model, as in many other models proposed for repetitive Ca²⁺ spiking, the period of sustained oscillations and waves decreases when the level of stimulation increases, in agreement with experimental observations. The model also predicts a decrease in the wave propagation velocity with increasing levels of stimulation, a question that still remains unsettled from an experimental point of view. The domain in $\nu_1\beta$ values explored in Fig. 9 *A* is bounded by two values of this parameter. Below $\nu_1\beta$ ≈ 0.2 μM min⁻¹, no propagating waves are observed. On the other hand, when $\nu_1\beta$ ≥ 1.05 μM min⁻¹, the behavior of the system becomes complex: the amplitude and velocity of successive Ca²⁺ fronts are highly variable and some of them vanish in the course of their propagation.

In contrast, increasing the Ca²⁺ influx from the external medium into the cytosol of *Xenopus* oocytes has been shown to increase both the frequency and the propagation velocity of the Ca²⁺ fronts (Girard and Clapham, 1993). Although in the homogeneous version of the model (i.e., neglecting diffusion of cytosolic Ca²⁺) both the influx from the outside (ν_0) and the release from the IP₃-sensitive store ($\nu_1\beta$) play a similar role, in the present situation, both parameters greatly differ in their spatial localization: $\nu_1\beta$ is locally applied at the left extremity of the system, while Ca²⁺ is supposed to enter (and quit) the system in an homogeneous manner in each point of the system. Such a situation is particularly appropriate for thin cells or for cases where the waves propagate near the plasma membrane. As a consequence, increasing the Ca²⁺ influx from the IP₃-sensitive pool ($\nu_1\beta$) or from the external medium (ν_0) has different effects (compare Fig. 9, *A* and *B*). Indeed, increasing the latter influx leads to a concomitant increase in the frequency and in the propagation
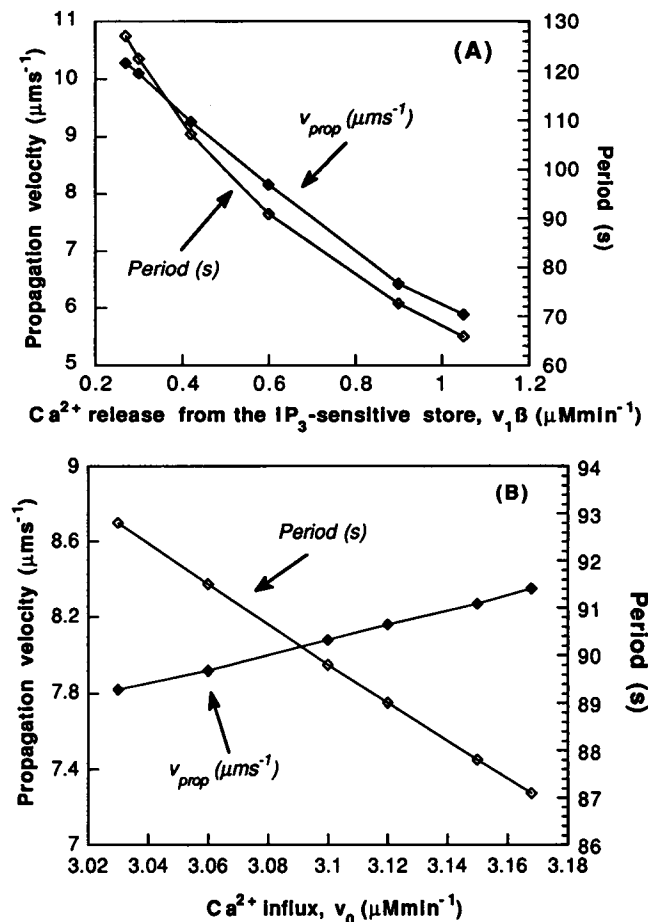
TABLE 1 Period (velocity) of Ca^{2+} waves of type 1 resembling those observed in *Xenopus* oocytes: effect of altering the maximum rate of Ca^{2+} pumping into the IP$_3$-insensitive store, V_{M2} (conditions are those of Fig. 8).

V_{M2} (μM min^{-1})	$v_1\beta(\mu$M min^{-1})	
	0.3	9.0
65	122.3 s (10.0 μm s^{-1})	103.8 s (9.0 μm s^{-1})
84	149.9 s (12.4 μm s^{-1})	53.7 s (4.9 μm s^{-1})

FIGURE 9   Period and velocity of Ca^{2+} waves of type 1 resembling those observed in *Xenopus* oocytes: effect of altering the rate of Ca^{2+} influx from the IP$_3$-sensitive store (*A*) or the influx of Ca^{2+} from the extracellular medium (*B*). Conditions are as in Fig. 8.

velocity of the Ca^{2+} fronts, in agreement with experimental observations in *Xenopus* oocytes (Girard and Clapham, 1993).

Finally, we have altered in our numerical simulations the maximal velocity of Ca^{2+} pumping into the stores (V_{M2}) to simulate the experiments performed by Camacho and Lechleiter (1993), in which they studied Ca^{2+} wave propagation in *Xenopus* oocytes expressing exogenous Ca^{2+}-ATPases. These authors observed that the period decreases as the rate of Ca^{2+} pumping rises, while the propagation rate remains roughly unchanged. The effect of parameter V_{M2} on the behavior of the model is complex and depends on the conditions considered. In the absence of Ca^{2+} diffusion (data not shown), the model based on CICR defined by Eqs. 1–4a predicts an increase in the period of oscillations when V_{M2} is increased, in contrast with experimental observations. This also occurs (see Table 1) when taking Ca^{2+} diffusion into account, as long as the stimulus applied at the left extremity of the system remains in the oscillatory domain defined by two critical levels of parameter β (see, e.g., Dupont et al., 1991). However, a significant increase in frequency with the rate of Ca^{2+} pumping into the stores is ob-

tained in the simulations (see Table 1) when the IP$_3$ level is large enough to bring the Ca^{2+} signaling system in the stimulated region largely above the oscillatory range. Under these conditions, a more rapid removal of cytosolic Ca^{2+} due to larger V_{M2} values will be associated with a higher frequency of Ca^{2+} oscillations farther away from the stimulated region. In the situation considered in Table 1, the decrease in period observed when increasing V_{M2} is quasi-discontinuous, with a sharp drop around $V_{M2} = 80$ μM min^{-1}. Moreover, as expected from the results shown in Fig. 9 *A*, a decrease in period is accompanied by a decrease in the velocity of the waves.

The present results provide an explanation for the experimentally observed increase in wave frequency in *Xenopus* expressing exogenous Ca^{2+}-ATPases, particularly in view of the fact that this effect is more pronounced at higher IP$_3$ levels (Camacho and Lechleiter, 1993).

PROPAGATING FRONTS AND SUSTAINED CA^{2+} WAVES OF TYPE 2

For Ca^{2+} fronts of type 2, a progressive rise of Ca^{2+} along the cell is followed by a quasi-homogeneous return to the basal level. Such fronts can also be simulated by the model based on CICR (Dupont and Goldbeter, 1992). From a theoretical point of view, for a given cell length, the difference between waves of types 1 and 2 stems from distinct velocities of the Ca^{2+} exchange processes between the cytosol, the external medium, and intracellular stores. Indeed, Ca^{2+} spikes characterized by a longer period and a larger half-width readily give rise to fronts of type 2 when Ca^{2+} diffusion is taken into account. Thus, the kinetics of Ca^{2+} exchange is much slower for waves of type 2 than for waves of type 1 when the dimension of the cell remains unchanged. In particular, V_{M2}, which represents the maximum rate of pumping of Ca^{2+} from the cytosol into the stores, plays a predominant role in determining the shape of the front: an increase in V_{M2} results in narrowing the Ca^{2+} spike in the course of time in each point of space. This result agrees with the experimental observation that spikes of cytosolic Ca^{2+} become narrower in *Xenopus* oocytes expressing additional Ca^{2+} ATPases (Camacho and Lechleiter, 1993).

Again, it must be emphasized that a continuum should exist between types 1 and 2 waves upon changing progressively the dimension of the cell.

Sustained Ca²⁺ Waves of Type 2

If the stimulation leading to a Ca²⁺ front of type 2 is maintained in a medium where Ca²⁺ pools are homogeneously distributed in the whole cell, periodic Ca²⁺ waves resembling those observed in hepatocytes are generated by the CICR model defined by Eqs. 1–4a. Fig. 10 shows the evolution of cytosolic Ca²⁺ concentration when using parameter values that optimize the qualitative agreement between the numerical simulations and the experimentally observed waves of type 2. Interestingly, the best agreement is obtained for phase waves, i.e., when all parts of the system oscillate but with different phases.

The typical aspect of waves of type 2 can be better characterized when following the time evolution of cytosolic Ca²⁺ at increasing distances from the stimulation site as shown in Fig. 11. There, one clearly sees that the rate of decrease of the Ca²⁺ level increases with the distance from the stimulation site; as a consequence, the return of the Ca²⁺ concentration occurs more or less uniformly in the whole system, in agreement with the observations by Thomas et al. (1991) on hepatocytes and with the numerical simulations performed by these authors by means of the present model based on CICR. In qualitative agreement with their experimental results (see Fig. 3 of their article) is the fact that the amplitude of the Ca²⁺ spike in the model is higher near the stimulation site, decreases farther away, and then increases again near the side opposed to stimulation. A slight difference between experiment and theory is nevertheless observed: in the experiments, the largest peak corresponds to
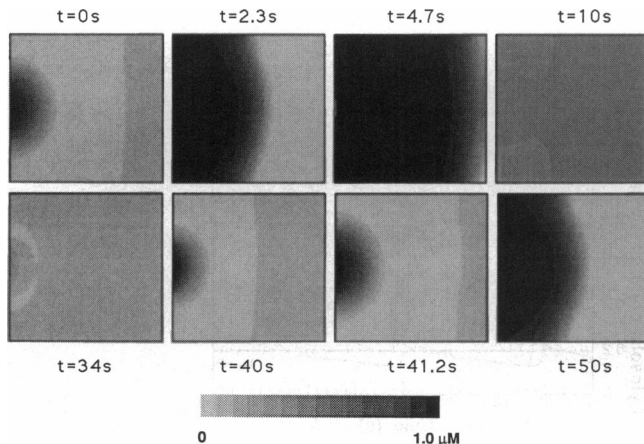

FIGURE 10   Ca²⁺ waves of type 2 generated by the model based on CICR. Cytosolic Ca²⁺ progressively rises throughout the cell, stays at an elevated plateau, and thereafter decreases in a quasi-homogeneous manner in the whole cell. The panels have been obtained by numerical simulations of Eqs. 1–4a with $v_0 = 1.8 \ \mu M \ min^{-1}$, $v_1\beta = 0$, $K_2 = 1 \ \mu M$, $V_{M2} = 93 \ \mu M \ min^{-1}$, $V_{M3} = 500 \ \mu M \ min^{-1}$, $K_R = 2 \ \mu M$, $K_A = 0.66 \ \mu M$, $k = 5.6 \ min^{-1}$, $k_f = 1 \ min^{-1}$ and $D_Z = 400 \ \mu m^2 \ s^{-1}$. The system, whose dimensions are 250 × 250 μm, is divided into a grid of 60 × 60 points. Continuous stimulation ($v_1\beta = 22.8 \ \mu M \ min^{-1}$) is applied in the central third of the first row on the left. In these conditions, the waves generated by the system are phase waves. The period and velocity of the Ca²⁺ wave are equal to 41 s and 53 $\mu m \ s^{-1}$, respectively.
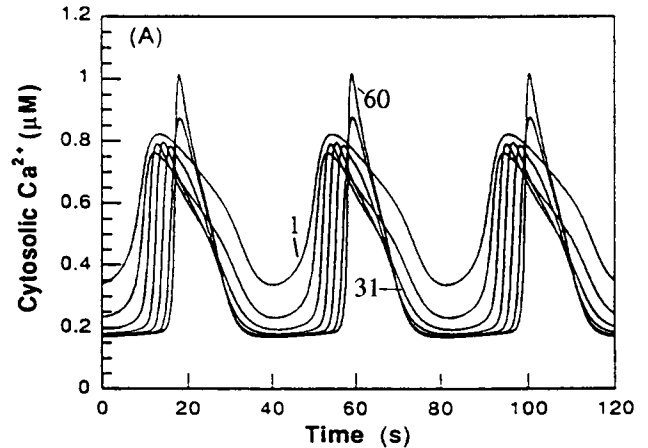

FIGURE 11   Temporal evolution of the cytosolic Ca²⁺ concentration in different locations in space in the situation corresponding to Fig. 10. The curves represent the time evolution of cytosolic Ca²⁺ in the middle of columns 1, 11, 21, 31, 51, and 60 of the spatial grid.

the initiation site of the wave while here the largest peak occurs at the opposite side of the cell.

Echo waves: role of boundary conditions

So far, we have considered the case where Ca²⁺ exchanges between the cytosol and the extracellular medium, taken into account through the terms v_0 and kZ (see Eq. 1), occur in all points of the system. Such a situation is particularly appropriate for thin cells. When these exchanges primarily take place at the borders, as should be the case for planar sections through thicker cells, echo waves are often observed in the numerical simulations. An example is shown in Fig. 12
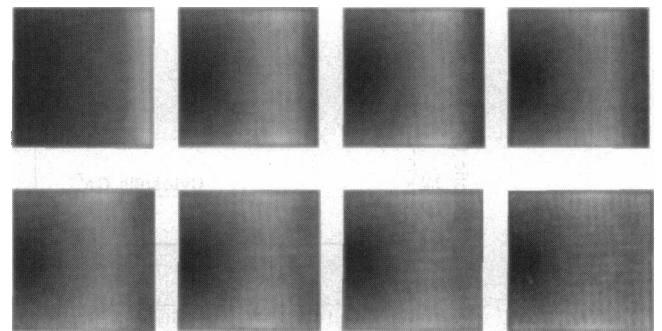

FIGURE 12   Echo wave of cytosolic Ca²⁺. The data are generated by the model based on CICR defined by Eqs. 1–4a. The panels represent eight successive images at 0.5 s intervals, 127 s after the onset of stimulation. The system of 250 × 250 μm is divided into a grid of 60 × 60 points. Constant stimulation ($v_1\beta = 10.8 \ \mu M \ min^{-1}$) is applied in the first left row of the system. Only the four border rows are assumed to exchange Ca²⁺ with the extracellular medium, through the terms v_0 and $-kZ$, which are omitted elsewhere in the evolution equations. Parameter values are $v_0 = 1.68 \ \mu M \ min^{-1}$, $V_{M2} = 93 \ \mu M \ min^{-1}$, $K_2 = 1 \ \mu M$, $V_{M3} = 500 \ \mu M \ min^{-1}$, $K_R = 2 \ \mu M$, $K_A = 0.66 \ \mu M$, $k = 18.8 \ min^{-1}$, $k_f = 1 \ min^{-1}$, and $D_Z = 400 \ \mu m^2 \ s^{-1}$. To allow for better visualization of the echo wave, the grey scale has been modified for each individual panel; in all cases, black corresponds to the maximum instantaneous Ca²⁺ concentration and white to the minimum.

where the initial wave stops before reaching the extremity of the cell opposed to the initiation site because an echo-wave has emerged from the distal side. There indeed, cytosolic Ca^{2+} concentration is high due to the influx from the extracellular medium and to Ca^{2+} accumulation owing to zero-flux boundary conditions at the membrane. This echo wave halts at a certain distance from the membrane because of the refractoriness of the regions through which the initial wave has traveled. Both the direct and the echo waves propagate at a velocity of about 15 μm s^{-1} in the case considered in Fig. 12. From an experimental point of view, echo waves of Ca^{2+} have been observed in ascidian eggs by Speksnijder et al. (1990).

CA^{2+} WAVES IN THE ONE-POOL MODEL

To study wave propagation in the one-pool model, the level of IP$_3$ can still be treated as a parameter. However, because IP$_3$ now behaves as a co-agonist for Ca^{2+} release, it is of particular interest to treat IP$_3$ as an additional variable to incorporate the effect of IP$_3$ diffusion. To this end, a third equation has to be added to Eq. 1 to describe the local evolution of IP$_3$ concentration. This equation takes the form

$$\frac{\partial A}{\partial t} = v_p R - k_d A + D_A \left(\frac{\partial^2 A}{\partial x^2} + \frac{\partial^2 A}{\partial y^2} \right) \qquad (6)$$

where A is the concentration of IP$_3$ and v_p the maximal rate of IP$_3$ production; R denotes the degree of PLC activation; k_d is an apparent first-order kinetic constant characterizing IP$_3$ degradation; D_A stands for the diffusion coefficient of IP$_3$, and x and y for the two spatial coordinates. Parameter β, which represents the saturation level of the IP$_3$ receptor in Eq. 2, can now be written as

$$\beta = \frac{A^3}{K_1^3 + A^3} \qquad (7)$$

where K_1 denotes the dissociation constant of the IP$_3$ receptor. The results of the simulations do not noticeably depend on the value of the Hill coefficient for IP$_3$ binding to the receptor; here this coefficient is taken equal to 3, in agreement with experimental observations (Meyer et al., 1988).

In the one-pool model, because Ca^{2+} and IP$_3$ behave as co-agonists for CICR, the wave only propagates when the IP$_3$ concentration exceeds a critical level throughout the cell. Such a situation is illustrated in Fig. 13. The level of IP$_3$ (bold line) decreases exponentially with the distance from the site of stimulation and rapidly reaches a constant value which, above a threshold, allows for sustained Ca^{2+} oscillations. Fig. 13, A and B, correspond respectively to situations where the IP$_3$ level lies below or above this threshold. That wave propagation requires a critical level of IP$_3$ has been established in *Xenopus* oocytes (DeLisle and Welsh, 1992; Lechleiter and Clapham, 1992).

The dashed line in Fig. 13 shows the evolution of the concentration of intravesicular Ca^{2+} near the stimulation site. The filling level of the Ca^{2+} store plays a predominant role in the timing of Ca^{2+} oscillations. Indeed, in the model, the decrease in intravesicular Ca^{2+} brings about the termination of the Ca^{2+} spike. It should be stressed that the pools are not empty after the occurrence of a spike. Given that in the model all concentrations are defined with respect to the total cell volume and that the pools occupy a volume that is about 10
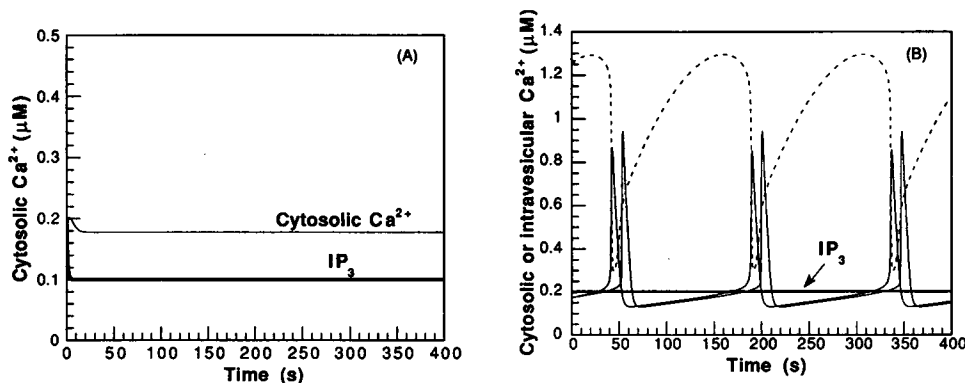

FIGURE 13   Influence of the IP$_3$ level on cytosolic Ca^{2+} waves in the one-pool model based on CICR. Propagation of sustained Ca^{2+} waves fails to occur when the level of IP$_3$ is too low (A) and only occurs when the IP$_3$ level is sufficiently large (B), even though the influx of extracellular Ca^{2+} (measured by v_0) remains the same in the two cases. The two panels only differ by the level of IP$_3$ established at steady state in the bulk of the cell; this level equals 0.1 mM in (A) and 0.2 mM in (B). The system of 250 × 250 μm is divided into a grid of 64 × 64 points. In panel (A), the evolution of the concentration of IP$_3$ and of cytosolic Ca^{2+} in the middle of the system are represented. In panel (B), the thin, solid curves represent the evolution of the cytosolic Ca^{2+} concentration at the two extremities of the cell, in points (1, 32) and (64, 32) of the spatial mesh; the bold and dashed lines represent, respectively, the IP$_3$ level and the intravesicular Ca^{2+} concentration in the first of these points. The curves have been obtained by numerical integration of eqs. (1–3, 4b, 5 and 6) with the following parameter values: $v_0 = 1.7$ μM min^{-1}, $v_1 = 3$ μM min^{-1}, $V_{M2} = 25$ μM min^{-1}, $K_2 = 0.5$ μM, $V_{M3} = 325$ μM min^{-1}, $K_R = 1$ μM, $K_A = 0.6$ μM, $k = 10$ min^{-1}, $k_f = 1$ min^{-1}, $v_p = 2$ μM min^{-1}, $k_d = 1$ min^{-1}, $K_1 = 0.1$ μM, $D_Z = 40$ μm^2 s^{-1}, and $D_A = 200$ μm^2 s^{-1}. Cell stimulation is achieved by setting parameter R equal to 0.7 in the central third of the first column of the mesh; everywhere else R is set equal to 0.05 in (A) and 0.1 in (B). For both panels, initial conditions have been chosen as the stable steady state obtained in panel (B) in the absence of stimulation.

times smaller than the cytosol, Fig. 13 shows that the concentration of free Ca^{2+} in the stores always largely exceeds that in the cytosol.

DISCUSSION

The present study shows that a one- or two-pool model based on CICR can account for Ca^{2+} oscillations and waves resembling those experimentally observed in a variety of cells. Because Ca^{2+} waves appear to behave differently in various cell types, it is of interest to try to understand the origin of these peculiarities. To this effect, we have used a theoretical approach to investigate questions such as the origin of qualitatively distinct types of waves and the incidence of the dimensions of the cell and of the spatial distribution of Ca^{2+} pools, as well as possible differences between the one- and two-pool versions of the model based on CICR.

Except for the effect on the amplitude and latency of the first spike, already observed for oscillations (Dupont and Goldbeter, 1993) and for the role of IP_3 (see below), we did not find any major differences between the behavior of the one- and two-pool versions of the model based on CICR with respect to Ca^{2+} wave propagation. Thus, the primary role played by the autocatalytic CICR regulation in the occurrence of Ca^{2+} oscillations is recovered for the propagation of intracellular waves. The influence of IP_3 on wave propagation nevertheless differs in the one- and two-pool versions of the CICR model. In the two-pool model, oscillations and waves can occur in the absence of IP_3, provided that the Ca^{2+} influx (v_0) from the external medium is sufficiently high. In contrast, for Ca^{2+} oscillations and waves to occur in the one-pool model based on IP_3-sensitive CICR, IP_3 has to exceed a critical level as demonstrated by the comparison of A and B in Fig. 13. The requirement for a sufficient level of IP_3 in wave propagation fits the observation that Ca^{2+} waves are suppressed in *Xenopus* oocytes injected with heparin (Lechleiter and Clapham, 1992) or antibodies against the IP_3 receptor (Miyazaki et al., 1992).

As previously emphasized for solitary Ca^{2+} fronts (Dupont and Goldbeter, 1992), it appears that the two types of waves, a steep Ca^{2+} increase propagating as a sharp band as in cardiac cells (waves of type 1), or a smoother rise followed by a quasi-homogeneous return to the basal level as in hepatocytes (waves of type 2) can readily be generated by the model, provided that the appropriate parameter values are used. The classification of waves into type 1 or 2 is nevertheless somewhat arbitrary, as a continuum likely exists between the two kinds of waves. Thus, imagining that one could sufficiently increase the length of a cell while retaining a period of oscillations on the order of 1 min, the progressive transition from a wave of type 1 into a wave of type 2 via intermediate patterns should be observed. Feasible is the converse experiment that consists in shortening the period of Ca^{2+} oscillations by overexpressing gene products such as Ca^{2+}-ATPases (Camacho and Lechleiter, 1993). Upon de-

creasing the period, Ca^{2+} waves should progressively change from type 2 to type 1.

We have first focused on type 1 fronts or waves, using successively cardiac myocytes and *Xenopus* oocytes as prototypes. The case of myocytes allowed us to investigate the effect of altering the distance between the CICR domains. It appears that the distribution of these domains markedly affects the propagation velocity of Ca^{2+} waves. This was shown here for waves of type 1 (Fig. 7), but a similar result should hold for waves of type 2. Such a conclusion agrees with observations indicating that the Ca^{2+} wave in oocytes propagates more rapidly in the animal pole, which contains more Ca^{2+} pools, than in the vegetal pole (see the theoretical study of Cheer et al., 1987). The results also hold with experimental observations showing that the propagation rate of the Ca^{2+} wave in pancreatic acinar cells decreases from 12 to 4 $\mu m\ s^{-1}$ as the density of Ca^{2+} pools decreases in distinct parts of the cell (Kasai et al., 1993). We further showed that waves of type 1 fail to propagate when the distance between successive Ca^{2+} pools falls below a few μm, which distance is on the order of the one apparent from the discrete structure of the sarcoplasmic reticulum in cardiac myocytes (Moses and Delcarpio, 1983).

A related, theoretical study of the impact of the distance between Ca^{2+} channels on the velocity of propagation of a Ca^{2+} wave along the surface of intracellular stores has led to a slightly different conclusion (Mironov, 1990). The distance between two successive channels that maximizes the propagation velocity is predicted in that study to be equal to 3 μm, instead of being nil as in the present study. This difference must be ascribed to the fact that Mironov considered the existence of a three-state Ca^{2+} channel (closed, open, and inactivated). Thus, a rapid return to the closed state is favored by some separation between two successive channels.

The distribution of Ca^{2+} pools also influences the relationship between stimulation and propagation velocity. The present study indicates that the propagation velocity of a Ca^{2+} front, or, equivalently, of the first wave of a train, depends only slightly on the stimulation level when the Ca^{2+} stores are distributed discretely throughout the cell. Although these results have been obtained for waves of type 1, they should also apply to waves of type 2. This result might explain why, in hepatocytes, the propagation velocity does not significantly vary with the concentration of external agonist (Thomas et al., 1991). The present results thus raise the possibility that differences as to the dependence of propagation velocity on external stimulation in pancreatic acinar cells, oocytes, and hepatocytes might originate from differences in the spatial distribution of Ca^{2+} pools.

The modeling of the type 1 waves encountered in *Xenopus* oocytes allowed us to investigate the effect of altering different kinetic parameters on the period and velocity of Ca^{2+} waves. Thus, we have changed successively v_0, the rate of Ca^{2+} influx from the extracellular medium, $v_1\beta$, the velocity of Ca^{2+} release from IP_3-sensitive stores, and V_{M2}, the maximum rate of Ca^{2+} pumping into Ca^{2+}-sensitive stores. The

model based on CICR could reproduce the experimentally observed behavior concerning an increase in period with increasing influx both from the extracellular medium and from the IP₃-sensitive store (Berridge, 1993). In contrast, how the velocity of the waves changes as a function of these parameters depends on the nature of the Ca^{2+} influx considered. In the model, a homogeneously increased influx of Ca^{2+} from the extracellular medium leads to a rise in the propagation velocity as observed after hyperpolarization of *Xenopus* oocytes (Girard and Clapham, 1993). However, if the increase is supposed to be localized at one extremity of the cell, to model the existence of functionally localized IP₃-sensitive pools, the model predicts a decrease in the velocity of propagation when Ca^{2+} influx is increased.

From an experimental point of view, the relationship between the stimulation level and the rate of propagation of the Ca^{2+} waves is still unclear and could vary from one cell type to another. Theoretically, it is easy to understand that a homogeneous increase of the baseline level of Ca^{2+} permits a more rapid local transition from the resting to the excited state and thus a more rapid propagation of the wave. In contrast, when only the pacemaker region receives an increased influx, its frequency is accelerated but one does not modify the properties of the system elsewhere. As the system has less time to fully recover its excitability between two successive fronts, the propagation velocity of the wave will decrease.

Finally, the influence of the rate of Ca^{2+} pumping has also been investigated using as prototypes Ca^{2+} waves resembling those observed in *Xenopus* oocytes. The analysis shows that, in contrast with the behavior of the homogeneous model, an acceleration of pumping may, in certain conditions, be accompanied by a rise in the frequency of the waves as seen in the experiments (Camacho and Lechleiter, 1993). The simulations predict that this result can only be obtained when the localized stimulus is such that the stimulated region of the cell remains at a very high, nonoscillating level of Ca^{2+}. It is thus a region near the stimulated one that enters the oscillatory domain and behaves as pacemaker. Upon increasing the rate of Ca^{2+} pumping into the stores, the system enters the oscillatory domain in a region closer to the stimulation layer, the pacemaker region is then subjected to a higher effective stimulus. Hence the decrease in period observed upon increasing parameter V_{M2} (see Table 1). The data indicate that beyond a certain point the frequency increases abruptly as a function of V_{M2}, an observation that calls for further theoretical analysis.

Waves of type 2, observed in hepatocytes or endothelial cells, have been described as those for which the width of the front is of the same order as, or larger than, the typical cell length. We have shown that, for a given cell length, the occurrence of such waves implies that the Ca^{2+} exchange processes are much slower than for waves of type 1. This hypothesis is corroborated by some experimental observations. Thus, astrocytes, whose size is approximately that of cardiac myocytes, which provide a prototype for type 1 waves, show waves of type 2 (Yagodin et al., 1994) probably because their Ca^{2+} exchange processes are slower than in the latter cell

type. Accordingly, the period of oscillations is of the order of 5–10 s in astrocytes, and <1 s in myocytes. In the same manner, *Xenopus* oocytes, in which the period of Ca^{2+} oscillations is of the order of tens of seconds, often display waves of type 1 because of their huge diameter, on the order of 1 mm (Camacho and Lechleiter, 1993).

On the other hand, it appears from the numerical simulations that, if the stimulation is maintained, the best qualitative agreement between observations performed on type 2 waves and the behavior of the model is obtained when all parts of the system are spontaneously oscillating with different phases, i.e., for phase waves. That some cell types may in certain conditions display Ca^{2+} phase waves is a working hypothesis that calls for further experimental and theoretical investigations.

When the volume of the cell is so large that Ca^{2+} fluxes between the cytosol and the extracellular medium only take place at the boundaries of the two-dimensional system in the present simulations, a phenomenon of echo wave is often observed (see Fig. 12). This phenomenon is due to the type of boundary conditions used. These conditions specify that Ca^{2+} cannot diffuse passively out of the system, the only efflux term being given by the apparent first-order process measured by the term $-kZ$ in Eq. 1. As a result, the concentration of cytosolic Ca^{2+} rises at the extremity of the cell opposed to the site of stimulation, thereby initiating a Ca^{2+} wave that travels in the opposite direction and stops when it reaches a zone of refractoriness left by the passage of the primary wave. Echo waves have been observed in ascidian eggs (Speksnijder et al., 1990).

In conclusion, it appears that much as for Ca^{2+} oscillations, a one- or two-pool model based on CICR is capable of accounting for a variety of experimental observations on intracellular Ca^{2+} waves when diffusion of cytosolic Ca^{2+} is incorporated into the kinetic equations. In particular, the model accounts for the two types of waves that have been experimentally observed. Using the two-pool CICR model, Girard et al. (1992) have shown that it can also reproduce spiral wave patterns such as those observed in *Xenopus* oocytes. It is likely that the model could similarly account for spiral waves recently observed in cardiac myocytes (Lipp and Niggli, 1993). The model has further been applied and extended to account for the intercellular propagation of Ca^{2+} waves (Sneyd et al., 1994).

The present results show that variations in properties of intracellular Ca^{2+} waves such as waveform, wavelength, propagation velocity, and period can be modulated by altering a number of factors such as the spatial distribution of intracellular Ca^{2+} pools, the dimension of the cell, or the kinetic parameters measuring the various Ca^{2+} exchange processes between the cytosol and intracellular stores. Of key importance for oscillations and waves of cytosolic Ca^{2+} is the destabilizing mechanism of CICR release. This conclusion holds whether that mechanism operates in the presence of two distinct Ca^{2+} pools, respectively sensitive to IP₃ or Ca^{2+}, or of a single Ca^{2+} pool sensitive to Ca^{2+} or to Ca^{2+} and IP₃ behaving as co-agonists for Ca^{2+} release.

REFERENCES

Allbritton, N., T. Meyer, and L. Stryer. 1992. Range of messenger action of calcium ion and inositol 1,4,5-trisphosphate. *Science.* 258:1812–1815.

Amundson, J., and D. Clapham. 1993. Calcium waves. *Curr. Opin. Neurobiol.* 3:375–382.

Atri, A., J. Amundson, D. Clapham, and J. Sneyd. 1993. A single pool model for intracellular calcium oscillations and waves in the *Xenopus laevis* oocyte. *Biophys. J.* 65:1727–1739.

Backx, P., P. De Tombe, K. Van Deen, B. Mulder, and J. Ter Keurs. 1989. A model of propagating calcium-induced calcium release mediated by calcium diffusion. *J. Gen. Physiol.* 93:963–977.

Berridge, M. J. 1990. Calcium oscillations. *J. Biol. Chem.* 268:9583–9586.

Berridge, M. J. 1993. Inositol trisphosphate and calcium signalling. *Nature.* 361:315–325.

Berridge, M. J., and G. Dupont. 1994. Spatial and temporal signalling by calcium. *Curr. Opin. Cell Biol.* 6:267–74.

Berridge, M. J., and A. Galione. 1988. Cytosolic calcium oscillators. *FASEB J.* 2:3074–3082.

Bezprozvanny, I., J. Watras, and B. Ehrlich. 1991. Bell-shaped calcium response curves of Ins(1,4,5)P₃- and calcium-gated channels from endoplasmic reticulum of cerebellum. *Nature.* 351:751–754.

Blatter, L. A., and G. Wier. 1992. Agonist-induced [Ca²⁺]ᵢ waves and Ca²⁺-induced Ca²⁺ release in mammalian vascular smooth muscle cells. *Am. J. Physiol.* H576–H586.

Boitano, S., E. Dirksen, and M. J. Sanderson. 1992. Intercellular propagation of calcium waves mediated by inositol trisphosphate. *Science.* 258:292–295.

Busa, W. B., J. E. Ferguson, S. K. Joseph, J. R. Williamson, and R. Nuccitelli. 1985. Activation of frog (*Xenopus laevis*) eggs by inositol trisphosphate. I. Characterization of Ca²⁺ release from intracellular stores. *J. Cell Biol.* 101:677–682.

Camacho, P., and J. Lechleiter. 1993. Increased frequency of Ca²⁺ waves in *X. laevis* oocytes expressing a Ca²⁺-ATPase. *Science.* 260:226–229.

Charles, A. C., J. Merrill, E. Dirksen, and M. J. Sanderson. 1991. Intercellular signaling in glial cells: calcium waves and oscillations in response to mechanical stimulation and glutamate. *Neuron.* 6:983–992.

Cheek, T. R., O. M. McGuinness, C. Vincent, R. B. Moreton, M. J. Berridge, and M. H. Johnson. 1993. Fertilization and thimerosal stimulate similar calcium spiking patterns in mouse oocytes but by separate mechanism. *Development.* 119:179–189.

Cheer, A., J. P. Vincent, R. Nuccitelli, and G. Oster. 1987. Cortical activity in vertebrate eggs. The activation wave. *J. Theor. Biol.* 124:377–404.

Cheng, H., W. J. Lederer, and M. B. Cannell. 1993. Calcium sparks: elementary events underlying excitation-contraction coupling in heart muscle. *Science.* 262:740–744.

Cornell-Bell, A., S. Finkbeiner, M. Cooper, and J. Smith. 1990. Glutamate induces calcium waves in cultured astrocytes: long range glial signalling. *Science.* 247:1143–1146.

Cuthbertson, K. S. R. 1989. Intracellular calcium oscillators. *In* Cell to Cell Signalling: From Experiments to Theoretical Models. A. Goldbeter, editor. Academic Press, London. 435–447.

Cuthbertson, K. S. R., and T. Chay. 1991. Oscillations in cell calcium. *Cell Calcium.* 12, number 2/3.

Cuthbertson, K. S. R., and P. Cobbold. 1991. The hepatocyte calcium oscillator. *Cell Calcium.* 12:97–110.

De Young, G., and J. Keizer. 1992. A single-pool inositol 1,4,5-trisphosphate-receptor-based model for agonist-stimulated oscillations in Ca²⁺ concentration. *Proc. Natl. Acad. Sci. USA.* 89:9895–9899.

DeLisle, S., and M. Welsh. 1992. Inositol trisphosphate is required for the propagation of calcium waves in *Xenopus* oocytes. *J. Biol. Chem.* 267:7963–7966.

Donnahue, B., and R. Abercrombie. 1987. Free diffusion coefficient of ionic calcium in cytoplasm. *Cell Calcium.* 8:437–448.

Dupont, G., M. J. Berridge, and A. Goldbeter. 1990. Latency correlates with period in a model for signal-induced Ca²⁺ oscillations based on Ca²⁺-induced Ca²⁺ release. *Cell Regul.* 1:853–861.

Dupont, G., M. J. Berridge, and A. Goldbeter. 1991. Signal-induced Ca²⁺ oscillations: properties of a model based on Ca²⁺-induced Ca²⁺ release. *Cell Calcium.* 12:73–86.

Dupont, G., and A. Goldbeter. 1992. Oscillations and waves of cytosolic calcium: insights from theoretical models. *BioEssays.* 14:485–493.

Dupont, G., and A. Goldbeter. 1993. One-pool model for Ca²⁺ oscillations involving Ca²⁺ and inositol 1,4,5-triphosphate as co-agonists for Ca²⁺ release. *Cell Calcium.* 14:311–322.

Endo, M., and M. Iino. 1990. Properties of calcium release channels of the intracellular calcium store in muscle cells. *In* The Biology and Medicine of Signal Transduction. Y. Nishizuka, editor, Raven Press, New York. 122–127.

Fewtrell, C. 1993. Ca²⁺ oscillations in non-excitable cells. *Annu. Rev. Physiol.* 55:427–454.

Finch, E., T. Turner, and S. Golden. 1991. Calcium as a coagonist of inositol 1,4,5-trisphosphate-induced calcium release. *Science.* 252:443–446.

Foskett, J., and D. Wong. 1991. Free cytoplasmic Ca²⁺ concentration oscillations in thapsigargin-treated parotid acinar cells are caffeine- and ryanodine-sensitive. *J. Biol. Chem.* 266:14535–14538.

Galione, A. 1992. Ca²⁺-induced Ca²⁺ release and its modulation by cyclic ADP-ribose. *Trends Pharmacol. Sci.* 13:304–306.

Galione, A., A. McDougall, W. B., Busa, N. Willmott, I. Gillot, and M. Whitaker. 1993. Redundant mechanisms of calcium-induced calcium release underlying calcium waves during fertilization of sea urchin eggs. *Science.* 261:348–352.

Girard, S., and D. Clapham. 1993. Acceleration of intracellular calcium waves in *Xenopus* oocytes by calcium influx. *Science.* 260:229–232.

Girard, S., A. Lückhoff, J. Lechleiter, J. Sneyd, and D. Clapham. 1992. Two-dimensional model of calcium waves reproduces the patterns observed in *Xenopus* oocytes. *Biophys. J.* 61:509–517.

Goldbeter, A., G. Dupont, and M. J. Berridge. 1990. Minimal model for signal-induced calcium oscillations and for their frequency encoding through protein phosphorylation. *Proc. Natl. Acad. Sci. USA.* 87:1461–1465.

Hoth, M., and R. Penner. 1992. Depletion of intracellular calcium stores activates a calcium current in mast cells. *Nature.* 355:353–355.

Jacob, R. 1990. Imaging cytoplasmic free calcium in histamine stimulated endothelial cells and in FMET-LEU-PHE stimulated neutrophils. *Cell Calcium.* 11:241–249.

Jaffe, L. F. 1983. Sources of calcium in egg activation: a review and hypothesis. *Dev. Biol.* 99:265–276.

Jaffe, L. F. 1993. Classes and mechanisms of calcium waves. *Cell Calcium.* 14:736–745.

Jafri, M., S. Vajda, P. Pasik, and B. Gillo. 1992. A membrane model for cytosolic calcium oscillations. A study using *Xenopus* oocytes. *Biophys. J.* 63:235–246.

Kasai, H., Y. X. Li, and Y. Miyashita. 1993. Subcellular distribution of Ca²⁺ release channels underlying Ca²⁺ waves and oscillations in exocrine pancreas. *Cell.* 74:669–677.

Kijima, Y., A. Saito, T. Jetton, M. Magnuson, and S. Fleisher. 1993. Different intracellular localization of inositol 1,4,5-triphosphate and ryanodine receptors in cardiomyocytes. *J. Biol. Chem.* 268:3499–3506.

Kort, A. A., M. C. Capogrossi, and E. G. Lakatta. 1985. Frequency, amplitude and propagation velocity of spontaneous Ca²⁺-dependent contractile waves in adult rat cardiac muscle and isolated myocytes. *Circ. Res.* 57:844–855.

Kuba, K., and S. Takeshita. 1981. Simulation of intracellular Ca²⁺ oscillation in a sympathetic neurone. *J. Theor. Biol.* 93:1009–1031.

Kushmerick, M., and R. Podolsky. 1969. Ion mobility in muscle cells. *Science.* 166:1297–1298.

Law, G., A. Pachter, O. Thastrup, R. Hanley, and P. Dannies. 1990. Thapsigargin, but not caffeine, blocks the ability of thyrotropin-releasing hormone to release Ca²⁺ from an intracellular store in GH₄C₁ pituitary cells. *Biochem. J.* 267:359–364.

Lechleiter, J., and D. Clapham. 1992. Molecular mechanism of intracellular calcium excitability in *X. laevis. Cell.* 69:283–294.

Lechleiter, J., S. Girard, E. Peralta, and D. Clapham. 1991. Spiral calcium wave propagation and annihilation in *Xenopus laevis* oocytes. *Science.* 252:123–126.

Lee, H. C., R. Aarhus, and T. F. Walseth. 1993. Calcium mobilization by dual receptors during fertilization of sea urchin eggs. *Science.* 261: 352–355.

Lipp, P., and E. Niggli. 1993. Microscopic spiral waves reveal positive feedback in subcellular calcium signaling. *Biophys. J.* 65:2272–2276.

Lipp, P., and E. Niggli. 1994. Modulation of Ca^{2+} release in cultured neonatal rat cardiac myocytes. *Circ. Res.* 74:974–990.

Matsumoto, T., H. Kanaide, Y. Shogakinchi, and M. Nakumura. 1990. Characteristics of the histamine-sensitive calcium store in vascular smooth muscle. *J. Biol. Chem.* 265:5610–5616.

Meldolesi, J., L. Madeddu, and T. Pozzan. 1990. Intracellular storage organelles in non-muscle cells: heterogeneity and functional assignment. *Biochim. Biophys. Acta.* 1055:134–140.

Meyer, T. 1991. Cell signaling by second messenger waves. *Cell.* 64: 675–678.

Meyer, T., and L. Stryer. 1988. Molecular model for receptor-stimulated calcium spiking. *Proc. Natl. Acad. Sci. USA.* 85:5051–5055.

Meyer, T., and L. Stryer. 1991. Calcium spiking. *Annu. Rev. Biophys. Biophys. Chem.* 20:153–174.

Meyer, T., D. Holowka, and L. Stryer. 1988. Highly cooperative opening of calcium channels by inositol 1,4,5-triphosphate. *Science.* 240: 653–656.

Mironov, S. L. 1990. Theoretical analysis of Ca wave propagation along the surface of intracellular stores. *J. Theor. Biol.* 146:87–97.

Miyazaki, S., M. Yuzaki, K. Nakada, H. Shirakawa, S. Nakanishi, S. Nakade, and K. Mikoshiba. 1992. Block of Ca^{2+} wave and Ca^{2+} oscillations by antibody to the inositol 1,4,5-triphosphate receptor in fertilized hamster egg. *Science.* 257:251–255.

Moses, R. L., and J. B. Delcarpio. 1983. Sarcoplasmic reticulum and intermediate filament organization in cultured neonatal cardiac muscle cells. *Cell Tissue Res.* 228:489–496.

Nathanson, M., P. Padfield, A. O'Sullivan, A. Burgstahler, and J. Jamieson. 1992. Mechanism of Ca^{2+} wave propagation in pancreatic acinar cells. *J. Biol. Chem.* 267:18118–18121.

Nathanson, M., A. Burgstahler, and M. Fallon. 1994. Multi-step mechanism of polarized Ca^{2+} wave patterns in hepatocytes. *Am. J. Physiol.* In press.

Parekh, A., H. Terlau, and W. Stühmer. 1993. Depletion of $InsP_3$ stores activates a Ca^{2+} and K^+ current by means of a phosphatase and a diffusible messenger. *Nature.* 364:814–817.

Parker, I., and Y. Yao. 1991. Regenerative release of calcium from functionally discrete subcellular stores by inositol triphosphate. *Proc. R. Soc. Lond.* B246:269–274.

Putney, J. 1991. Capacitive calcium entry revisited. *Cell Calcium.* 11: 611–624.

Randriamampita, C., and R. Y. Tsien. 1993. Emptying of intracellular Ca^{2+} stores releases a novel small messenger that stimulates Ca^{2+} influx. *Nature.* 364:809–814.

Rooney, T. A., and A. P. Thomas. 1993. Intracellular calcium waves generated by Ins(1,4,5)P_3-dependent mechanisms. *Cell Calcium.* 14: 674–690.

Sneyd, J., A. Charles, and M. Sanderson. 1994. A model for the propagation of intercellular calcium waves. *Amer. J. Physiol.* In press.

Sneyd, J., S. Girard, and D. Clapham. 1993. Calcium wave propagation by Ca^{2+}-induced Ca^{2+} release: an unusual excitable system. *Bull. Math. Biol.* 55:315–344.

Somogyi, R., and J. Stucki. 1991. Hormone-induced calcium oscillations in liver cells can be explained by a simple one pool model. *J. Biol. Chem.* 266:11068–11077.

Speksnijder, J., C. Sardet, and L. Jaffe. 1990. Periodic calcium waves cross ascidian eggs after fertilization. *Dev. Biol.* 142:246–249.

Stauderman, K., and M. Murawsky. 1991. The inositol 1,4,5-triphosphate-forming agonist histamine activates a ryanodine-sensitive Ca^{2+} release mechanism in bovine adrenal chromaffin cells. *J. Biol. Chem.* 266: 19150–19153.

Stern, M. D. 1992. Theory of excitation-contraction coupling in cardiac muscle. *Biophys. J.* 63:497–517.

Swillens, S., and D. Mercan. 1990. Computer simulation of a cytosolic calcium oscillator. *Biochem. J.* 271:835–838.

Takamatsu, T., and B. Wier. 1990. Calcium waves in mammalian heart: quantification of origin, magnitude, waveform and velocity. *FASEB J.* 4:1519–1525.

Thomas, A., D. Renard, and T. Rooney. 1991. Spatial and temporal organization of calcium signalling in hepatocytes. *Cell Calcium.* 12: 111–126.

Tsien, R. W., and R. Y. Tsien. 1990. Calcium channels, stores and oscillations. *Annu. Rev. Cell Biol.* 6:715–760.

Tyson, J., and J. Keener. 1988. Singular perturbation theory of travelling waves in excitable media (a review). *Physica D.* 32:327–361.

Wakui, M., Y. V. Osipchuk, and O. H. Petersen. 1990. Receptor-activated cytoplasmic Ca^{2+} spiking mediated by inositol triphosphate is due to Ca^{2+}-induced Ca^{2+} release. *Cell.* 63:1025–1032.

Wakui, M., B. Potter, and O. H. Petersen. 1989. Pulsatile intracellular Ca^{2+} release does not depend on fluctuations in inositol triphosphate concentration. *Nature.* 339:317–320.

Walton, P., J. Airey, J. Sutko, C. Beck, G. Mignery, T. Südhof, T. Deerinck, and M. Ellisman. 1991. Ryanodine and inositol triphosphate receptors coexist in avian cerebellar Purkinje neurons. *J. Cell Biol.* 113:1145–1157.

Whitaker, M., and R. F. Irvine. 1984. Inositol 1,4,5-triphosphate microinjection activates sea urchin eggs. *Nature.* 312:636–639.

Wong, A., A. Fabiato, and J. Bassingthwaigthe. 1992. Model of calcium-induced calcium release mechanism in cardiac cells. *Bull. Math. Biol.* 54:95–116.

Woods, N. M., K. S. R. Cuthbertson, and P. H. Cobbold. 1987. Agonist-induced oscillations in cytoplasmic free calcium in single rat hepatocytes. *Cell Calcium.* 8:79–100.

Yagodin, S., L. Holtzclaw, C. Sheppard, and T. Russell. 1994. Nonlinear propagation of agonist-induced cytoplasmic calcium waves in single astrocytes. *J. Neurobiol.* 25:265–280.